

Routing with Classical Corrugated Waveguide Low-Pass Filters with Embedded Bends

Fernando Teberio^{1, *}, Jon M. Percaz¹, Ivan Arregui¹, Petronilo Martin-Iglesias², Txema Lopetegi¹, Miguel A. G. Laso¹, and Israel Arnedo¹

Abstract—A very simple design method to embed routing capabilities in classical corrugated filters is presented in this paper. The method is based on the calculation of the heights and lengths of the so-called filters design building blocks, by means of a consecutive and separate extraction of their local reflection coefficients along the device. The proposed technique is proved with a 17th-order Zolotarev-filter whose topology is bent twice so that the input and output ports are in the same plane while preserving the in-line filters behaviour. This new filter allows the possibility of eliminating subsequent bending structures, reducing the insertion loss, weight, and PIM.

1. INTRODUCTION

The physical configuration of numerous applications such as ground terminals or multi-beam satellite payloads has become very intricate in order to allocate different RF/microwave components which are put together trying to make the best use of the volume available. In ground terminals, it is easy to find complex structures with low-pass filters and bends which are conveniently allocated to obtain a more compact terminal [1–3]. Multi-beam payloads are triggering the need of very compact output sections because up to hundreds of waveguide filters and bends are used to accomplish different functions [4]. In fact, once a signal has been amplified, it needs to be filtered and channelized/combined depending on the terminal/payload configuration [5]. Nowadays, when the physical configuration of the terminal/payload needs a bend before or after the low-pass filter, two different structures are utilized. This issue produces a negative impact in terms of insertion loss, volume/mass, and passive intermodulation (PIM) if we compare it with the solution presented in this paper. Therefore, developing a novel design technique for waveguide filters with adaptable physical layout will improve the industry's freedom to trade-off all these variables, and it will also boost the flexibility to design more complex and compact terminals and payloads.

The classical corrugated low-pass filters in rectangular waveguide technology have been widely employed in previous applications. Indeed, its design method is very well explained in [6] and available in commercial software tools. Very recently, an analytical approach has been proposed to accurately obtain their final physical dimensions using exclusively closed-form expressions [7]. As far as the authors' knowledge, all efforts to fold waveguide filters have kept focused on band-pass filters [8, 9]. In the case of low-pass filters, all of them follow the same in-line topology as in [7], and, typically, if a classical corrugated low-pass filter with embedded bends is required, its frequency response is retrieved by brute-force optimization of the constituent physical parameters, using only the optimizer tool of an electromagnetic software (i.e., FEST3D for instance). However, this paper goes beyond that and presents a very simple design technique that could be easily implemented in a software tool (i.e.,

Received 22 February 2018, Accepted 24 March 2018, Scheduled 9 April 2018

* Corresponding author: Fernando Teberio (fernando.teberio@unavarra.es).

¹ Electrical and Electronic Engineering Department, UPNA Pamplona E-31006, Spain. ² European Space Agency (ESA), European Space Research and Technology Centre (ESTEC), 2200 AG Noordwijk, The Netherlands.

FEST3D, CST MWS, etc.) to obtain directly a bent filter with the required routing specifications, which would be very practical for the satellite community to avoid further optimization, additional bending structures and the connection between them.

In this paper, a design method for bended topologies of the classical corrugated low-pass filters in rectangular waveguide is presented as an example of a new class of filters with routing capabilities. The novel method (Section 2) provides a simple modular design which could be easily integrated in an electromagnetic (EM) software design module, allowing designers to obtain routing low-pass filters with or without bends, avoiding subsequent bending structures and reducing insertion loss, volume/weight, and PIM. The novel topology and the design method have been validated thorough a 17th-order Zolotarev filter with two embedded bends (Section 3).

2. DESIGN METHOD

The design method begins by calculating the electrical step-impedance prototype, consisting of $N + 2$ transmission lines with electrical length θ and different characteristic impedances Z_i , for a chosen all-pole frequency response of order N . The Z_i values are calculated by applying the well-known Richards transformation and the UE (Unit Element) extraction procedure, fully detailed in [6]. Then, the local reflection coefficients, Γ_i , produced in each step between two UEs by the Z_i mismatch, are calculated following Eq. (1).

$$\Gamma_i = \frac{Z_{i+1} - Z_i}{Z_{i+1} + Z_i} \quad (1)$$

The combination of all these Γ_i placed θ -rad apart produces the intended frequency response of the low-pass filter [7].

The novel design technique utilizes a divide-and-rule strategy. Thus, instead of paying attention to the whole structure, the constituent Design Building Blocks (DBBs) will be calculated separately and consecutively, to eventually assemble the filter afterwards. The i th-DBB is composed of the second half of the i th-waveguide section, the first half of the $(i + 1)$ th-section, and the junction between them, as in Fig. 1. See Fig. 1(a) for a straight DBB and Fig. 1(b) for a folded DBB.

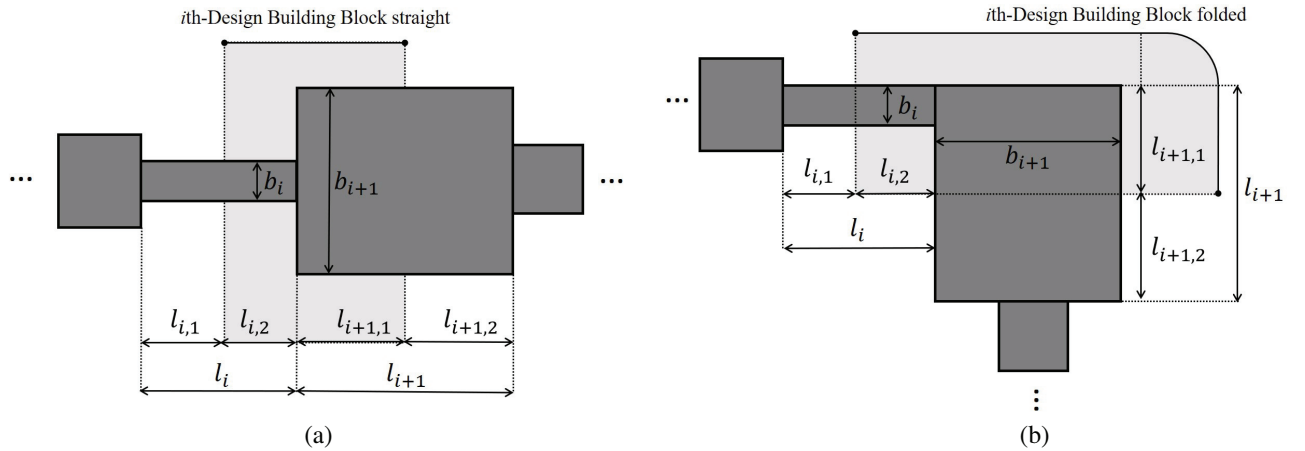


Figure 1. Detailed notation of an i th-DBB and their associated constituent parameters: (a) Sketch of the in-line topology where the second waveguide section is connected straight. (b) Sketch of the folded topology where the second waveguide section is connected downwards.

Reproduced courtesy of the Electromagnetics Academy

The procedure for obtaining the dimensions of each DBB will be the same, regardless of the type of junction between the contiguous sections (straight, folded up- or down-wards). In particular, the DBB should behave as its electrical model prototype composed of one-half transmission line, an impedance step, and another one-half transmission line. We could then connect two waveguide sections using an in-line or a folded configuration, depending on the desired final layout, while the response is preserved.

Firstly, b_1 is set. This value is usually established in accordance to the requirements of power handling and out-of-band performance. Then, b_2 is computed to satisfy that $|S_{11,1}(f_c)| = |\Gamma_1|$, where $|S_{11,1}(f_c)|$ is the magnitude of the S_{11} -parameter of the 1st-DBB at the passband upper frequency, f_c . This magnitude value only depends on the heights b_1 and b_2 , and since b_1 has already been fixed, b_2 can be easily obtained by means of an EM software tool (where high-order modes are taken into account). Notice that if $\Gamma_i > 0$, then $b_i < b_{i+1}$, and if $\Gamma_i < 0$, then $b_i > b_{i+1}$. Then, proceeding consecutively with the rest of the DBBs, once a certain b_i is known, b_{i+1} is calculated to assure that $|S_{11,i}(f_c)|$ provides the reflection value prescribed by $|\Gamma_i|$. When $i = N + 1$, all b_i s in the final structure have been calculated.

The design process continues with the calculation of length l_i of each waveguide section. As aforementioned and can be observed in Figs. 1(a) and (b), we consider both halves of two consecutive waveguide sections as the DBB. Hence, in the i th-DBB, two different lengths will be computed, i.e., $l_{i,2}$ (second half of the i th-section) and $l_{i+1,1}$ (first half of the $(i+1)$ th-section). Both lengths will be calculated taking into account the phase of the i th-DBB, in transmission, $\phi_{i,S_{21}}$, and in reflection, $\phi_{i,S_{11}}$, to resemble the target. On the one hand, the phase of the i th-DBB in transmission should satisfy:

$$\phi_{i,S_{21}}(f_c) = -\theta_c \quad (2)$$

where θ_c is the target electrical length at the passband upper frequency, f_c . On the other hand, depending on the sign of the targeted Γ_i , the i th-DBB reflection phase should satisfy:

$$\phi_{i,S_{11}}(f_c) = 180 - \theta_c \quad \text{for } b_i < b_{i+1} \quad (3)$$

$$\phi_{i,S_{11}}(f_c) = -\theta_c \quad \text{for } b_i > b_{i+1} \quad (4)$$

Notice that those phases are affected by the high-order modes excited in the vicinity of each junction, but we can compute $l_{i,2}$ and $l_{i+1,1}$ using again an EM simulator, as done in the b_i calculations.

Summarizing, the novel design method allows designers to obtain the filters physical structure with an aimed arbitrary topology and whose frequency response will be very close to the desired one in a negligible CPU time. A minor adjustment can be needed only in the lengths of the final prototype, accounting for the effect of high-order modes excited in the junctions, which are evanescently present in the intersections of the DBBs, and the slight frequency dependence of the reflection coefficient of the junction. Then, the final structure ready to be fabricated is accomplished. Finally, it is important to note that the aim of this filter is to suppress the fundamental TE_{10} mode in the rejected band (as in the in-line counterpart). If the suppression of the higher order TE_{n0} modes was required, a waveguide width modification could be also included following the same idea as in [10].

3. DESIGN EXAMPLE

In order to demonstrate the feasibility of the novel design technique proposed in this paper, a corrugated waveguide low-pass filter with routing capability will be designed. The novel filter will fulfil the following frequency specifications: passband from 10 GHz to 10.8 GHz with in-band return loss of 20 dB, and stopband between 13 GHz and 15 GHz with attenuation level of 60 dB. In this example, the standard input and output WR75 ports are required to be placed at the same plane (see Fig. 2). A Zolotarev function of order 17, passband lower frequency $f_{Zolo} = 8.1$ GHz, $f_c = 11$ GHz, in-band return loss

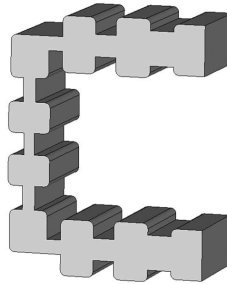


Figure 2. 3D view of the desired filter.
Reproduced courtesy of the Electromagnetics Academy

of 23 dB, $f_0 = 15$ GHz, and port dimensions $a = 19.05$ mm and $b = 9.525$ mm (WR75 standard) are considered.

With these parameters and [7] the in-line solution is achieved very accurately (grey line in Fig. 3). If the filter is directly bended to fit the pursued volume allocation, the frequency response is completely distorted (black line in Fig. 3). Following instead the method described in Section 2, using Equations (1) to (4), and FEST3D to simulate each DBB, we can obtain all b_i and l_i in the filter. All physical dimensions are detailed in Table 1, and the frequency response is shown in grey line in Fig. 4. As can be seen, a very good starting point for the final adjustment is directly accomplished. Optimizing a little bit only the lengths the final structure is achieved, see black line in Fig. 4.

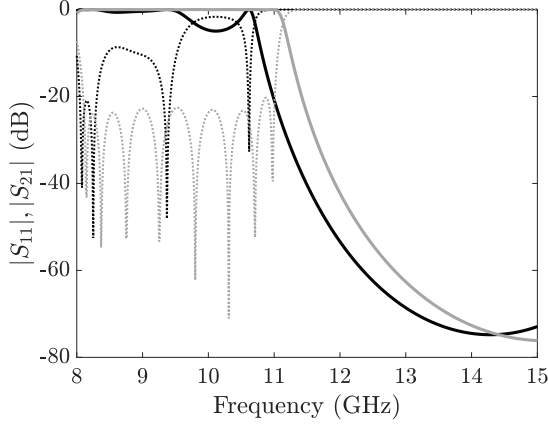


Figure 3. FEST3D simulated frequency response comparison between the in-line design (grey line) and the directly bent counterpart in junctions 6 and 13 (black line). $|S_{11}|$ in dotted line and $|S_{21}|$ in solid line.

Reproduced courtesy of the Electromagnetics Academy

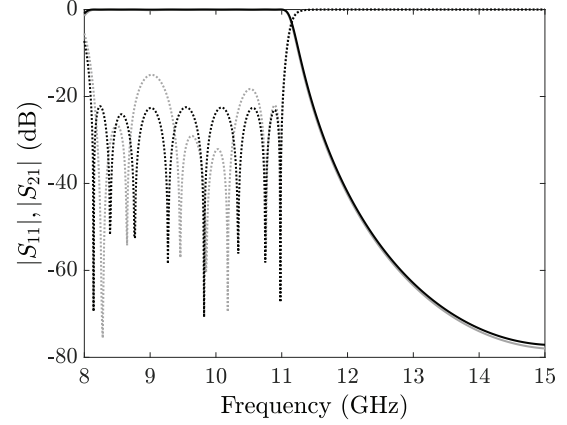


Figure 4. FEST3D simulated frequency response comparison between the novel filter designed with the technique in Section 2 without (grey line) and with the final adjustment (black line). $|S_{11}|$ in dotted line and $|S_{21}|$ in solid line.

Reproduced courtesy of the Electromagnetics Academy

Table 1. Final dimensions of the novel filter with embedded bends.

UEs	Z_i	Height, b_i (mm)	Length, l_i (mm)	i -DBB
1, 19	1.000	9.525	5.000	
2, 18	0.687	6.580	4.5	straight
3, 17	1.160	10.974	6.607	straight
4, 16	0.433	4.189	4.006	straight
5, 15	1.110	10.533	6.400	straight
6, 14	0.307	2.974	3.168	straight
7, 13	0.920	7.797	7.616	folded-down
8, 12	0.242	2.071	3.272	straight
9, 11	0.797	6.798	7.805	straight
10	0.221	1.895	3.365	straight

Finally, as a matter of clarity and as can be observed in Fig. 5(a) (direct comparison between grey line Fig. 3 and black line Fig. 4), there is no significant difference in the stopband when we excite both the in-line and the bent filter with the fundamental TE_{10} mode. Moreover, as can be seen in Fig. 5(b), the same higher-order TE_{n0} frequency response is obtained for both the in-line and the bent waveguide low-pass filter (frequency range plotted from 16 GHz up to 20 GHz). The higher-order non- TE_{n0} modes are not shown in the figure since their rejections are above 150 dB. Hence, there is no additional limitation in terms of higher-order mode excitation in the routing filter compared to that in

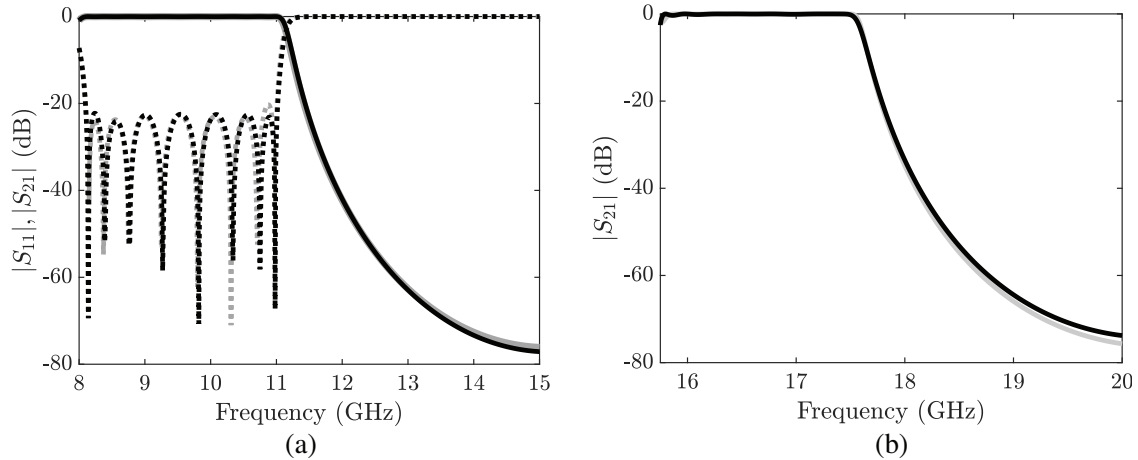


Figure 5. FET3D simulated frequency response comparison for the in-line design (grey line) and the novel filter in this paper (black line) for the (a) fundamental TE_{10} mode and (b) TE_{20} mode (the rest of the higher-order modes up to 20 GHz are below -150 dB). $|S_{11}|$ in dotted line and $|S_{21}|$ in solid line. Reproduced courtesy of the Electromagnetics Academy

its in-line counterpart.

The novel filter has been fabricated in aluminium in two halves in clam-shell configuration to reduce also the PIM of the structure (Fig. 6). The measurement results shown in Fig. 7 are very close to the simulated ones, and the filter fulfils not only the required frequency specifications but also the physical restrictions imposed.

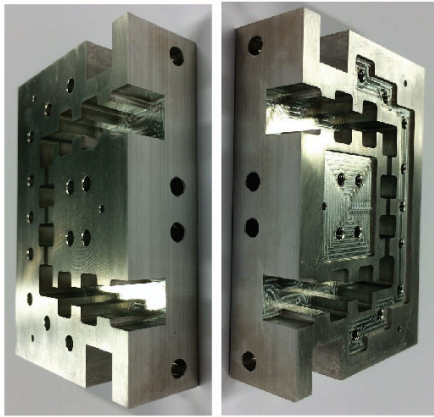


Figure 6. Photograph of the unassembled fabricated prototype.

Reproduced courtesy of the Electromagnetics Academy

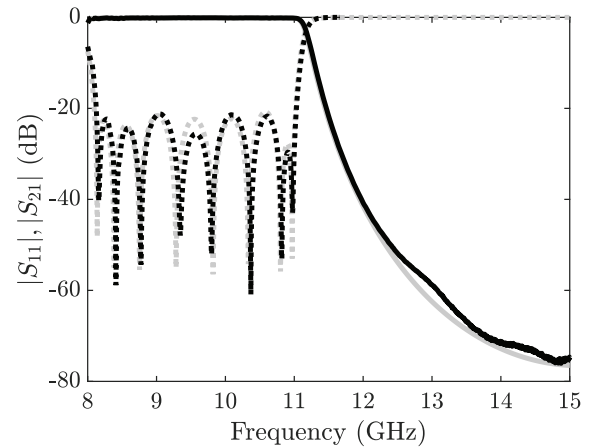


Figure 7. Frequency response measurements of the novel filter (black line) and CST MWS simulation of the novel filter with rounded corners (grey line). $|S_{11}|$ in dotted line and $|S_{21}|$ in solid line.

Reproduced courtesy of the Electromagnetics Academy

4. CONCLUSIONS

In this paper, a new easy and quick design technique to embed bends in classical corrugated waveguide low-pass filters has been proposed. This avoids cumbersome sub-assemblies reducing the insertion loss, weight, and PIM in ground terminals and multi-beam payloads. The proposed technique has been proved with a 17th-order Zolotarev bent filter whose frequency response measurements are very close to the simulated and targeted ones.

ACKNOWLEDGMENT

This work was supported by MINECO (Spain) (grant TEC2014-55735-C3-R, TEC2014-51902-C2-2-R, and TEC2017-85529-C3-2-R). The authors wish to thank Pablo Soto (UPV-Valencia, Spain) for the help with the numerical implementation of the Zolotarev function.

REFERENCES

1. Moheb, H., et al., "Design & development of co-polarized Ku-band ground terminal system for very small aperture terminal (VSAT) application," *IEEE APS-S*, Vol. 3, 2158–2161, 1999.
2. Avramis, E., et al., *Cross-polar and Co-polar Transceiver*, U.S. Patent 7474173 B2, Jun. 27, 2006.
3. Laidig, D., et al., *Integrated Waveguide Transceiver*, U.S. Patent 8433257 B2, Apr. 30, 2013.
4. Wolf, H., et al., "Satellite multi-beam antennas at airbus defense and space: State of the art and trends," *Proc. EuCAP*, 182–185, 2014.
5. Wang, J., et al., "A wideband waveguide diplexer for the extend c-band antenna systems," *Progress In Electromagnetics Research C*, Vol. 69, 73–82, 2016.
6. Cameron, R., et al., *Microwave Filters for Communication Systems: Fundamentals, Design and Applications*, John Wiley & Sons, Hoboken, NJ, 2007.
7. Teberio, F., et al., "Accurate design of corrugated waveguide low-pass filters using exclusively closed form expressions," *Proc. Eur. Microw. Conf.*, 182–185, 2017.
8. Morini, A., et al., "Curved filters in rectangular waveguide," *Proc. Eur. Microw. Conf.*, 182–185, 1996.
9. Carceller, C., et al., "Design of hybrid folded rectangular waveguide filters with transmission zeros below the passband," *IEEE Trans. Microw. Theory Tech.*, Vol. 64, No. 2, 475–485, 2016.
10. Levy, R., "Inhomogeneous stepped-impedance corrugated waveguide low-pass filters," *IEEE MTT-S Digest*, 2005.